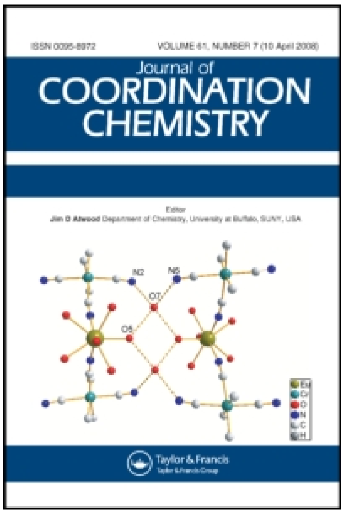

Journal of Coordination Chemistry
Publication details, including instructions for authors and subscription information:
http://www.informaworld.com/smpp/title~content=t713455674

Phase polymorphism of $[Ni(DMSO)_6](BF_4)_2$ studied by differential scanning calorimetry

A. Migdał-Mikuli[a]; Ł. Skoczylas[a]; E. Szostak[a]
[a] Faculty of Chemistry, Department of Chemical Physics, Jagiellonian University, Ingardena 3, 30-060 Kraków, Poland

To cite this Article Migdał-Mikuli, A. , Skoczylas, Ł. and Szostak, E.(2008) 'Phase polymorphism of $[Ni(DMSO)_6](BF_4)_2$ studied by differential scanning calorimetry', Journal of Coordination Chemistry, 61: 14, 2197 — 2206
To link to this Article: DOI: 10.1080/00958970801913860
URL: http://dx.doi.org/10.1080/00958970801913860

Journal of Coordination Chemistry
Vol. 61, No. 14, 20 July 2008, 2197–2206

Taylor & Francis
Taylor & Francis Group

Phase polymorphism of $[Ni(DMSO)_6](BF_4)_2$ studied by differential scanning calorimetry

A. MIGDAŁ-MIKULI*, Ł. SKOCZYLAS and E. SZOSTAK

Faculty of Chemistry, Department of Chemical Physics, Jagiellonian University,
Ingardena 3, 30-060 Kraków, Poland

(*Received 15 June 2007; in final form 27 July 2007*)

The tetrafluoroborate of hexadimethylsulfoxidenickel(II) was synthesized and studied by differential scanning calorimetry. Seven solid phases of $[Ni(DMSO)_6](BF_4)_2$ were revealed. Specifically, six phase transitions of the first order were detected between the following solid phases: stable KIb → stable KIa at $T_{C6} = 335$ K, metastable KIIb → metastable KIIa at $T_{C5} = 368$ K, metastable KIII → overcooled phase KI at $T_{C4} = 378$ K, metastable KIIa → overcooled phase KI at $T_{C3} = 396$ K, stable KIa → stable KI at $T_{C2} = 415$ K and stable KI → stable K0 at $T_{C1} = 433$ K. $[Ni(DMSO)_6](BF_4)_2$ begins decomposition at 440 K with loss of one DMSO molecule per formula unit forming $[Ni(DMSO)_5](BF_4)_2$ (phase L0) which melts next in two steps in the temperature range 550–593 K. From the entropy changes connected both with melting and with phase transitions, it can be concluded that phases KI, overcooled KI and K0 are orientationally dynamically disordered (ODIC) crystals. Stable phases KIb, KIa and metastable phase KIII are ordered solid phases. Metastable phase KIIa and metastable phase KIIb are more or less ordered solid phases.

Keywords: Hexadimethylsulfoxidenickel(II) tetrafluoroborate; Phase transitions; Melting point; DSC

1. Introduction

Hexadimethylsulfoxidenickel(II) tetrafluoroborate (called HNiTF) consists of $[Ni((CH_3)_2SO)_6]^{2+}$ and BF_4^-. The cation is a slightly deformed octahedron with nickel surrounded by six oxygens from dimethylsulfoxide (DMSO). Unfortunately, the crystal structure of HNiTF is unknown. However, $[Ni(DMSO)_6](ClO_4)_2$ crystallizes in the trigonal system (space group: No. 159; P31c; C_{3v}) [1, 2]. We have recently investigated the polymorphism of $[Ni(DMSO)_6](ClO_4)_2$ by DSC [3] and found six solid phases. From these measurements we concluded that four were stable and two were metastable. Phases K0 and overcooled K0 are orientationally dynamically disordered crystals. The stable phases KI, KIa, KIb and the metastable phases KII and KIII are more or less ordered solids.

The aim of this work was to examine the polymorphism of $[Ni(DMSO)_6](BF_4)_2$ at 97–440 K range using differential scanning calorimetry (DSC) and compare it with that of the hexadimethylsulfoxidenickel(II) perchlorate(VII).

---

*Corresponding author. Email: migdalmi@chemia.uj.edu.pl

Journal of Coordination Chemistry
ISSN 0095-8972 print/ISSN 1029-0389 online © 2008 Taylor & Francis
DOI: 10.1080/00958970801913860

2. Experimental

2.1. *Sample preparation*

A few grams of $[Ni(H_2O)_6](BF_4)_2$ were dissolved while being slowly heated in DMSO of high chemical purity [4], which was additionally purified by vacuum distillation at low pressure. This solution was then chilled and the precipitated crystals of HNiTF were filtered and washed with acetone. They were then dried in a desiccator over phosphorus pentoxide for a few hours. After desiccation, they were put in a sealed vessel and stored in a desiccator with barium oxide as a desiccant. To check the chemical composition of the synthesized HNiTF, the percentage content of nickel was checked using a complexometric method with a solution of the sodium salt of ethylenediaminetetraacetic acid (EDTA) as titrant. The carbon and hydrogen content was determined using elemental analysis on a EURO EA 3000 apparatus. The theoretical content of nickel is 8.37% and its found content was $8.3 \pm 0.1\%$. For carbon, the difference between the theoretical value (20.56%) and the test value ($20.64 \pm 0.01\%$) did not exceed 0.1% and the theoretical value for hydrogen was 5.18%, experimental $5.06 \pm 0.01\%$. Therefore, the elemental analysis confirmed six DMSO molecules in the complex cation.

2.2. *Sample characteristics*

In order to further identify the title compound, its infrared absorption spectra (FT-FIR and FT-MIR) and its Raman spectrum (FT-RS) were recorded at ambient temperature. The FT-FIR and FT-MIR spectra were made using Digilab FTS-14 and EQUINOX-55 Bruker Fourier transform infrared spectrometers, respectively, with a resolution of $2\,\mathrm{cm}^{-1}$. The FT-FIR spectrum of powder samples, suspended in apiezon grease, was recorded using polyethylene and silicon windows. The FT-MIR spectrum was recorded for a sample suspended in Nujol between KBr pellets. The FT-RS spectrum was recorded using a Bio-Rad spectrometer with a YAG neodymium laser ($\lambda = 1064\,\mathrm{nm}$) at 10–$4000\,\mathrm{cm}^{-1}$ with a resolution of $4\,\mathrm{cm}^{-1}$. All spectra were assigned based on literature data [4–8]. In addition to bands for $(CH_3)_2SO$, there were also bands at 98, 133, 187 and $244\,\mathrm{cm}^{-1}$, which can be assigned to $\nu_d(NiO)$, $\nu_s(NiO)$, $\delta_d(NiOS)$ and $\nu_s(NiO)$ vibrations, respectively. Thus, the spectra identify the compound as $[Ni(DMSO)_6](BF_4)_2$. Differential thermal analysis (DTA) and thermogravimetric (TG) measurements were performed using a Mettler Toledo TGA/SDTA 851e apparatus. A sample weighing 21.0421 mg was placed in a 70 μL corundum crucible. The thermogravimetric measurements were made in a flow of argon ($80\,\mathrm{mL\,min}^{-1}$) from 293 K up to 705 K at a constant heating rate of $10\,\mathrm{K\,min}^{-1}$. The temperature was measured by a Pt–Pt/Rh thermocouple with the accuracy of $\pm 0.5\,\mathrm{K}$. During heating to 440 K the sample loses only ca 2% of its initial mass, indicating that the compound does not change composition, even when the sample is not hermetically closed.

2.3. *Heat flow measurements*

At first we checked the phase polymorphism in the title compound using a Perkin-Elmer Pyris 1 DSC apparatus at 93–435 K for sample of mass 13.32 mg (sample A).

However, major DSC measurements of HNiTF were made at 293–435 K using a Mettler–Toledo 821e apparatus. Two samples of 10.98 mg (sample B) and 7.45 mg (sample C) were measured, each hermetically closed in 40 μL aluminum container. After the measurements masses of the samples did not change.

3. Results and discussion

DSC curves were obtained for each of three HNiTF samples A, B and C, at different scanning rates and at different initial and final sample heating and cooling conditions. We did not notice any differences between the results obtained for the particular samples. The thermodynamic parameters of the phase transitions are presented in table 1. The results of all DSC measurements are also schematically presented as a temperature dependence of the free enthalpy *G* (Gibbs free energy) and shown in all figures.

Measurements on A were started by cooling from room temperature (*RT*) to 93 K, holding at this temperature for 1 min, and next heating to 293 K. Both while cooling and while heating the sample from 93–293 K no anomalies on the DSC curves were recorded, indicating no phase transitions at this temperature region.

While heating sample B, with the scanning rate of 20 K min^{-1} (curve No 1), being initially in the KIb phase, from 273 to 435 K, a phase transition into an intermediate phase, named KIa, can be observed at $T_{C6} = 335$ K as a small and broad anomaly on DSC curve No. 1. Phase KIa next transforms into KI at $T_{C2} = 415$ K as a big anomaly on the same curve. Lastly, the KI phase transforms into high temperature phase K0 at $T_{C1} = 433$ K (see figure 1a and compare with scheme on figure 1b).

While cooling the sample from 435 K with a scanning rate of 20 K min^{-1} (in the K0 phase), it transforms to the stable phase KI at T_{C1}. As can be seen in figure 1a (DSC curve No. 2), when the sample is cooling, part of the overcooled KI phase (phase KI′) experiences a phase transition at $T_{C3} = 396$ K into phase KIIa. On further cooling, part of the sample in phase KI′ experiences phase transition at $T_{C4} = 378$ K to a metastable phase, called KIII, manifested by a big anomaly on the DSC curve. Part of the sample in the metastable phase KIIa has a phase transition at $T_{C5} = 368$ K to the metastable phase KIIb. It is difficult to see on curve No. 2 (see also the insert) an anomaly connected with this phase transition because only a very small part of the sample exists in phase KIIa (most is in phase KIII) and the enthalpy change

Table 1. Thermodynamic parameters of phase transitions in [Ni(DMSO)$_6$](BF$_4$)$_2$.

	[Ni(DMSO)$_6$](BF$_4$)$_2$		
	T_c (K)	ΔH (kJ mol^{-1})	ΔS (J mol^{-1} K^{-1})
T_{C6}	335 ± 1	1.27 ± 0.25	3.94 ± 0.76
T_{C5}	368 ± 1	1.68 ± 0.19	4.56 ± 0.52
T_{C4}	378 ± 1	30.22 ± 1.49	79.84 ± 3.76
T_{C3}	396 ± 1	24.86 ± 1.11	62.74 ± 3.25
T_{C2}	415 ± 1	40.49 ± 2.15	97.57 ± 5.22
T_{C1}	433 ± 1	1.90 ± 0.40	4.38 ± 0.95

connected with this phase transition is very small. On further cooling, the metastable KIII phase undergoes a spontaneous transformation into the metastable phase KIIb and also to the stable KIb as a small and broad anomaly on the DSC curve at 305 K (see figure 1a). Figure 1b shows schematically the *G versus T* dependence which presents the polymorphism discovered in DSC curves No. 1 and 2.

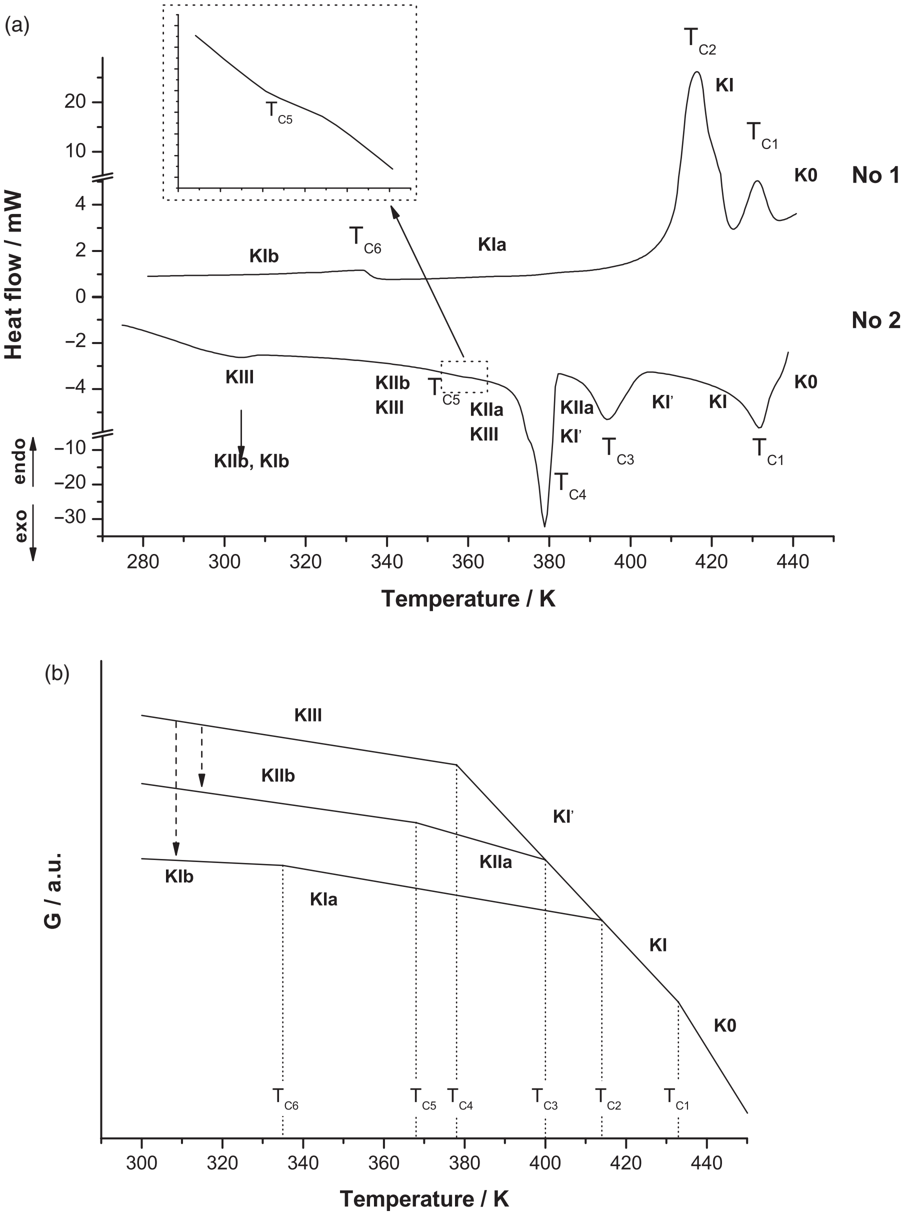

Figure 1. (a) DSC curves obtained during heating HNiTF from RT to 435 K (curve No. 1) and cooling at 435–273 K (curve No. 2) with a scanning rate of 20 K min^{-1}. (b) Phase polymorphism of HNiTF deduced from figure 1(a) DSC curves.

Heating B with a scanning rate of $20\,\mathrm{K\,min^{-1}}$ gives DSC curve No. 3 (figure 2a). Part of the sample in KIb transforms by an endothermic process into KIa at T_{C6} (small and broad endothermic anomaly on the DSC curve); the rest of the sample in metastable KIIb transforms at T_{C5} to the metastable KIIa, which next transforms at T_{C3} to KI′ (see the insert). When heating of B is continued, the transition from KIa to

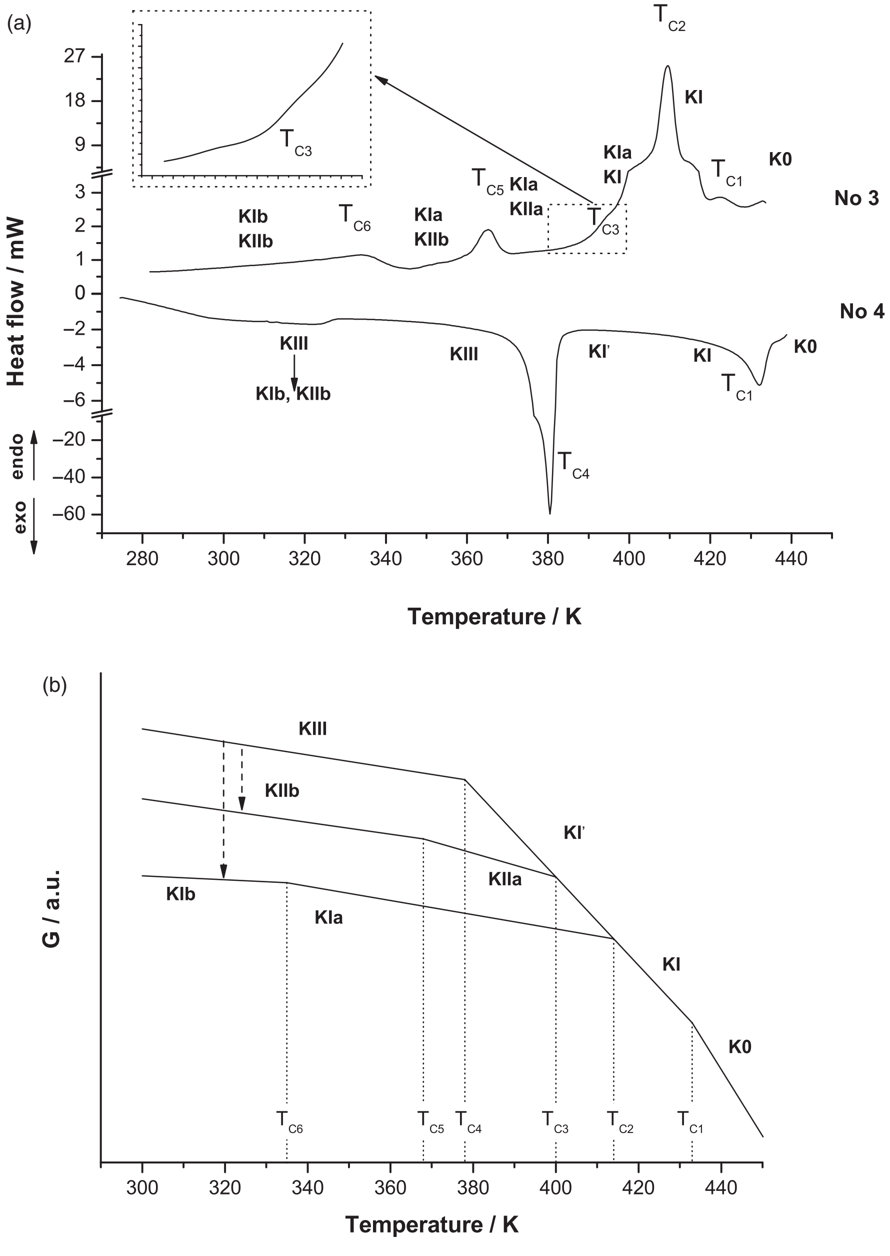

Figure 2. (a) DSC curves obtained during heating HNiTF from RT to 435 K (curve No. 3) and during cooling at 435–273 K (curve No. 4) with a scanning rate of $20\,\mathrm{K\,min^{-1}}$. (b) Scheme of HNiTF phase polymorphism deduced from figure 2(a) DSC curves.

KI at T_{C2} (big endothermic anomaly) and the transition from KI to K0 at T_{C1} take place (small anomaly). The onset of the anomaly at T_{C2} is at lower temperature than presented in figure 1. It is connected with phase transition KIIb → KIIa in $T_{C3} = 400\,\mathrm{K}$. Cooling of the sample with a scanning rate of $20\,\mathrm{K\,min^{-1}}$ gives curve No. 4, presented in figure 2(a). The K0 phase is cooled from 435 K transforming first to KI and then becomes deeply overcooled (phase KI′) transforming at T_{C4} to the metastable phase KIII. KII and KIII are monotropic phases. As shown in figure 2(a) (DSC curve No. 4), continuing cooling induces spontaneous transformation of the metastable phase KIII into KIb and KIIb at ca 320 K (very broad exothermic anomaly). Figure 2(b) shows schematically the G *versus* T dependence which presents the polymorphism on DSC curves No. 3 and 4.

Heating C in the temperature range 273–435 K gave the same results as in figure 1a (curve No. 1). Cooling sample C is shown in figure 3(a) (curve No. 5) with an anomaly connected with a phase transition from K0 to KI at T_{C1}. Next, the sample becomes overcooled (phase KI′) with a phase transition of a part of KI′ to KIIa at T_{C3} and finally transition of remaining part of KI′ to the metastable KIII at T_{C4}. Cooling was stopped before transformation of KIII to KIIb and to KIb, which usually took place at ca 320–300 K. Holding the sample at 358 K for 1 min and heating to 435 K gave DSC curve No 6, showing transition of KIIa to overcooled KI at T_{C3} (big endothermic peak); at a little higher temperature part of the overcooled KI converts in an exothermic process to the stable phase KIa. When heating is continued, the transition from KIa to KI at T_{C2} occurs (small broad anomaly). It is much smaller than analogous transitions on curve No. 1 or 3 because most of the sample remains in KI′. We do not see an anomaly connected with KI → K0 (it is too small). Evidently when the sample was held at 358 K, the spontaneous phase transition KIII → KIIb occurred.

Using a microscope, it was observed that all seven phases were solid phases. Our observations were confirmed by analyzing the DSC curve presented in figure 4. There are three anomalies between 460 K and 500 K, probably connected with decomposition and loss of one DMSO; continued heating gave three further anomalies from 570–620 K, with two connected with melting and the third with final decomposition.

It is not possible to determine the nature of observed phases only from DSC measurements. However, the change of the entropy of transitions ΔS (see table 1) suggests that phases KI, overcooled KI and K0 are orientationally dynamically disordered phases. Investigations by complementary methods, like X-ray diffraction, are now in progress.

The polymorphism of HNiTF is similar to that of $[\mathrm{Ni(DMSO)_6}](\mathrm{ClO_4})_2$ (called HNiC) [3] (see figure 5) and the phase transition parameters are similar. However, the most important difference is that all metastable phases of HNiTF are connected with overcooling of KI (but not K0, as observed in HNiC). Moreover, the HNiTF possesses one more metastable phase, namely the KIII phase.

4. Conclusions

(1) The thermodynamic parameters for the following phase transitions of HNiTF have been determined:

- reversible phase transition: stable KIb → stable KIa at $T_{C6} = 335\,\mathrm{K}$.

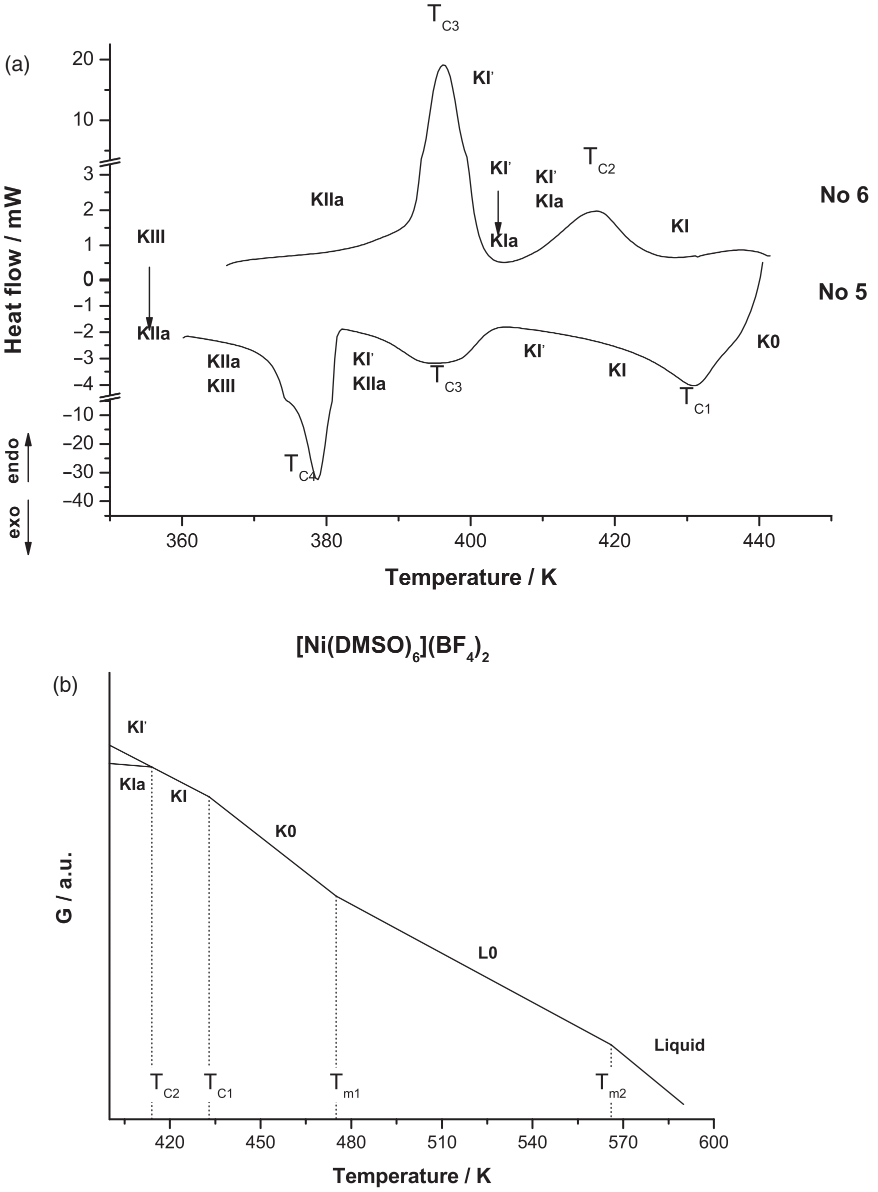

Figure 3. (a) DSC curves obtained during cooling HNiTF from 435–358 K (curve No. 5) and during heating at 358–435 K (curve No. 6) with a scanning rate of 20 K min^{-1}. (b) Scheme showing HNiTF phase polymorphism from DSC curves in figure 3(a).

- reversible phase transition: metastable KIIb → metastable KIIa at $T_{C5} = 368$ K.
- irreversible phase transition: metastable KIII → overcooled KI (KI′) at $T_{C4} = 378$ K.
- reversible phase transition: metastable KIIa → overcooled KI (KI′) at $T_{C3} = 396$ K.

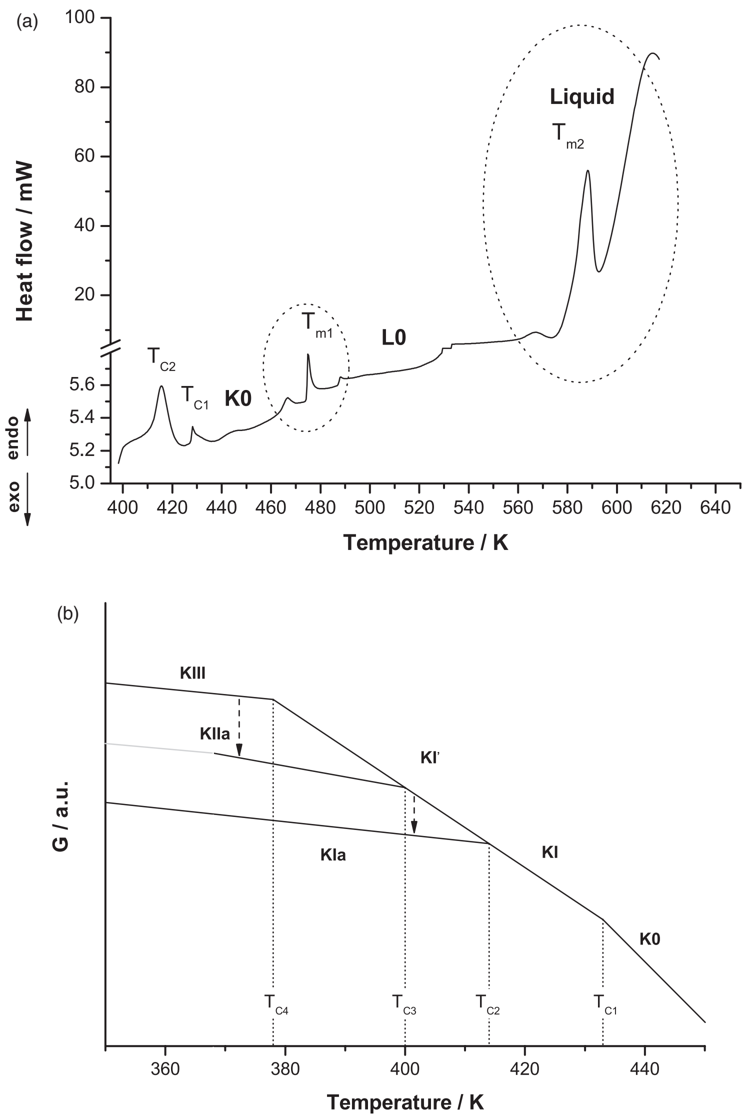

Figure 4. (a) DSC curve obtained during heating HNiTF from 400–650 K (curve No. 7) with a scanning rate of 20 K min^{-1}. (b) HNiTF phase polymorphism deduced from DSC curves in figure 4(a).

- irreversible phase transition: stable KIa → stable KI at $T_{C2} = 415$ K.
- reversible phase transition: stable KI → stable K0 at $T_{C1} = 433$ K.

(2) The entropy changes of the melting point and of the phase transitions indicate that KI, overcooled KI and K0 are likely "orientationally dynamically disordered crystals" (ODDIC), whereas the stable phases KIa, KIb and the metastable phases KIIa, KIIb and KIII are orientationally ordered solid phases.

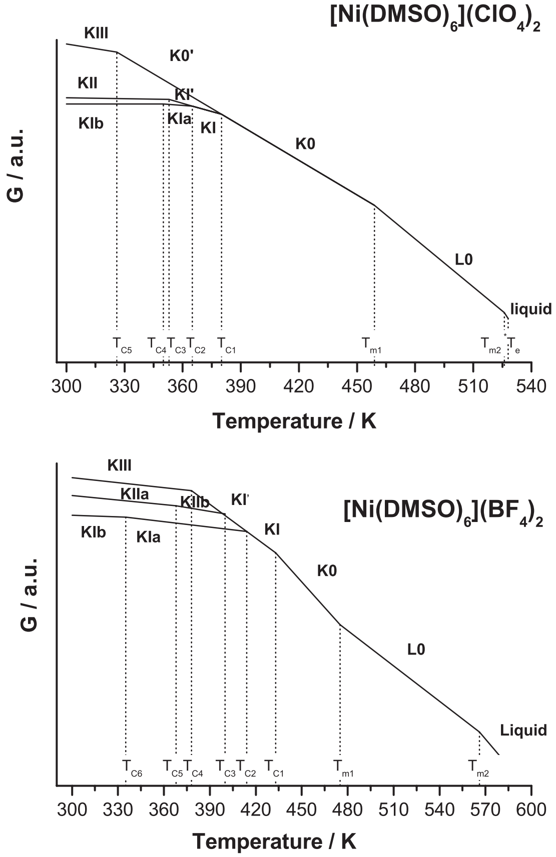

Figure 5. Comparison between the phase polymorphism of $[Ni(DMSO)_6](BF_4)_2$ and in $[Ni(DMSO)_6](ClO_4)_2$ [3].

(3) Phase polymorphism of the title compound has some differences to $[Ni(DMSO)_6](ClO_4)_2$.

Acknowledgement

Our thanks are due to Professor E. Mikuli from the Faculty of Chemistry, Jagiellonian University, for stimulating the discussion.

References

[1] E.J. Chan, B.G. Cox, J.M. Harrowfield, M.I. Ogden, B.W. Skelton, A.H. White. *Inorg. Chim. Acta*, **357**, 2365 (2004).

[2] M. Calligaris, O. Corugo. *Coord. Chem. Rev.*, **153**, 83 (1996).

[3] A. Migdal-Mikuli, E. Szostak. *Z. Naturforsch.*, **62a**, 67 (2007).
[4] J. Selbin, W.E. Bull, L.H. Holmes Jr. *J. Inorg. Nucl. Chem.*, **16**, 219 (1961).
[5] F.A. Cotton, R. Francis, W.D. Horrocks Jr. *J. Phys. Chem.*, **64**, 1534 (1960).
[6] M. Sandström, I. Persson, St. Ahrland. *Acta Chem. Scand. A*, **32**, 607 (1978).
[7] J.E. Connet, J.A. Creighton, J.H.S. Green, W. Kynaston. *Spectrochim. Acta*, **22**, 1859 (1966).
[8] Raman & IR Atlas, Verlag Chemie GmbH, Weinheim, Bergstr. (1974).